

## CHARACTERISATION OF LOCAL AL-BSF FORMATION FOR PERC SOLAR CELL STRUCTURES

F.S. Grasso<sup>1</sup>, L. Gautero<sup>1</sup>, Jochen Rentsch<sup>1</sup>, Ralf Preu<sup>1</sup> and R. Lanzafame<sup>2</sup>

<sup>1</sup>Fraunhofer Institute for Solar Energy Systems (ISE)  
Heidenhofstrasse 2, 79110 Freiburg, Germany

Phone: +49 (0)761-4588-5567, Email: federico.sebastiano.grasso@ise.fraunhofer.de,

<sup>2</sup>Università degli Studi di Catania, Facoltà di Ingegneria, Dipartimento di Ingegneria Industriale e Meccanica (DIIM)  
Viale Andrea Doria 6, 95125 Catania, Italy

**ABSTRACT:** Silicon wafers still represent a significant part of the costs of current solar modules. Passivated Emitter and Rear Cells (PERC) are a very promising technology in comparison to conventional cells. In this study PERC point like contacts at the back surface of p-type CZ silicon wafers realized with an industrial feasible technique are investigated. Since the formation of the Back Surface Field (BSF) is a critical step for the performance of solar cells, cross sections of the local contacts have been analyzed at the Scanning Electron Microscope (SEM). In order to investigate how to control the formation of the BSF, two different pastes consisting of pure aluminium particles were screen printed and different thermal profiles were applied. As a function of the width of the contacts, three major profiles can be observed: triangular, trapezoidal and with rounded edges at the sides. An explanation of the origin of these profiles is offered here. Concerning the results, one of the pastes allows achieving thicker and more homogenous BSF layers for widths of the contacts in the range of 120 to 190  $\mu\text{m}$ . This investigation shows that the present optical characterization is helpful to characterize the thickness of the BSF and, hence, its synergic use with electrical investigations can bring about enhancements in the performance of the cells.

**Keywords:** Back-Surface-Field, Screen Printing, Back Contact, Silicon Solar Cell, PERC, Inkjet.

### 1. INTRODUCTION

Currently, silicon is the most common material used for the large-scale production of solar cells, but wafers still represent a significant part of the costs of current solar modules. According to [1], lower  $W_{\text{peak}}$  prices can be achieved by increasing the performance of the cells and, simultaneously, by decreasing the consumption of silicon in the manufacturing of the wafers. In this context, Passivated Emitter and Rear Cells (PERC) represent a very promising technology since they are industrially feasible on thin wafers [2]. Anyway, PERC cells can become an alternative to the conventional solar cells only if their improved performances are obtained at comparable production costs. At their state of the art, conventional industrial cells and PERC cells present a similar front surface but a different rear surface. The former cells present a continuous interface between silicon and metal (usually Al). Instead, on the latter, local contacts are realized on to allow a significant amount of surface to be passivated. Three main contacting techniques are industrially feasible. These differentiate in the process, the first employs an inkjet masking [3], the second a dielectric ablation by means of laser [4] and the third uses a laser fired contacts approach [5]. The first technique will be investigated in this work.

For aluminium pastes a model of the contact formation is largely detailed in [6]. This model details a screen-printed paste on a bare silicon surface and subsequently fired at a high temperature in a Rapid Thermal Process (RTP) furnace. According to this model, the formed contact between silicon and aluminium consists of a stratification of three different layers. Starting from the aluminium side we find the fired paste, a newly formed eutectic alloy and an underlying epitaxial growth of silicon. This latter is grown on the already present silicon. In contrast to the existing silicon, the new layer is highly doped with aluminium. Hence, a high-low junction ( $p^+-p$ ) is formed [7]. In a solar cell this junction is better known as Back Surface Field (BSF) when located on the back surface. This built-in field, when properly formed, behaves like an electrical mirror for the

minority carriers and can reduce the surface recombination velocity (SRV) at the contact ([8] and [9]).

Similar studies concerning the formation of local contacts have already been detailed for LA in [10] and [11] whereas specific investigation on contacts are also present for the laser fired contact case [12]. Concerning Inkjet, the formation of point like contacts at the back surface has been investigated by the authors [13] for screen printed metallization. In that analysis a model of the alloying process is detailed according to the binary phase diagram of aluminium and silicon. Figure 1 shows the six different steps which lead to the formation of an oven fired local contact. The BSF results in a thin layer which grows epitaxially on the substrate on cooling down (steps 5 and 6).

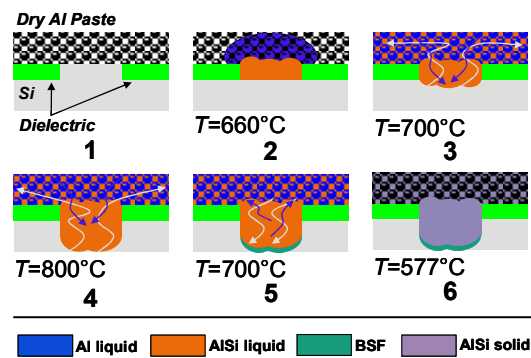


**Figure 1:** Sketch of the local contact formation during a RTP (from [13]).

The present study moves in the same direction as [13]. In addition, it steps forward by investigating how it is possible to control the formation of the local back surface field for Inkjet structured local contacts.

The analysis is carried out on silicon substrates which are treated with the same techniques used for the realization of solar cells. The rear surface of the wafer is properly structured in order to realize point like contacts at the back surface.

## 2. EXPERIMENTAL DETAILS

For the characterization p-type pseudo square CZ silicon wafers with a resistivity of  $3\pm 6 \Omega\text{cm}$  and a thickness of  $200 \mu\text{m}$  were used.

In Figure 2 the order of the processes applied to the wafers is shown.



**Figure 2:** The process flow shows the processing steps.

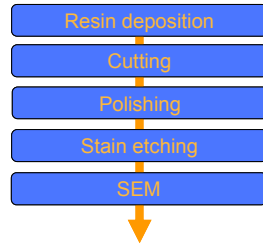


**Figure 3:** The process flow shows the sequence of the post-treatments.

First of all a saw damage etching step was performed with a dip in a hot 20%-KOH solution. Then a silicon nitride layer ( $\text{SiN}_x$ ) was deposited on the front surface of the wafers where neither a texture nor an emitter is present. The back surface of the wafers was passivated by depositing silicon nitride on top of an aluminium oxide ( $\text{AlO}_x$ ) stack. After depositing the passivation layer, both surfaces of the wafers were covered with an inkjet-printed wax. The front surface was fully masked whereas, on the rear surface, the mask presented windows with a well-defined geometrical pattern, optimized for the IJ-printing process [3]. In this regard the windows in the wax are squared with a side length of  $70 \mu\text{m}$ . The orientation of the opened windows is not aligned with the direction of the crystal easiest cleaving. It was observed that the cleaving axis of the crystal is  $45^\circ$  oriented respect to the edges of the wafers whereas the masking deposition was aligned to one of the sides of the wafer (see Figure 4).

After depositing the wax, the wafers were dipped in a 20%-HF solution in order to open windows in the passivation layer. After stripping the masks the measured openings of the dielectric resulted larger than expected. In this regard, circular windows with a diameter of  $150\pm 24 \mu\text{m}$  were observed.

The metallization process was performed by screen printing two different metallic pastes on the whole rear surface of the wafers. Both pastes consist of aluminium particles spread in a matrix of solvents which does not contain glass frits or any other compound useful to enhance the mechanical properties of the fired paste. All the wafers were screen printed with an amount of  $6 \text{ mg/cm}^2$  of wet paste.

After screen printing, the metallisation was dried in a thermal process in order to remove the solvents and then addressed to the firing in a RTP furnace.

Since it is known that the firing can affect the BSF formation [14], a thermal profile variation has been performed.

The characterization is based on a SEM analysis of

the thickness of the BSF as a function of the paste used and of the width of the local contacts.

Therefore, after processing the wafers, the samples are post-treated in order to obtain high quality cross sections of the local contacts. The post-treatments applied to the samples are described in the sketch of Figure 3.

A resin is spread on top of the metallization to preserve it during the further post-treating steps. Specimens are cut out of the processed samples with a dicing saw. The cut is then polished by means of argon ion beams.

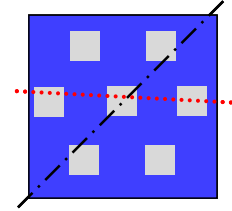


**Figure 4:** Sketch not in scale of the rear surface of the wafer. The passivation is indicated in blue, the cleaving axis is represented by the black line and a generic eventual sawing is indicated in red.

As already explained in [15], a stain etching technique is used to unveil the Al-doped regions in the substrate.

In conclusion these additional steps allow displaying the whole stratification of the contact at a scanning electron microscope (SEM). The thickness of the stain etched area is of interest. This observed doped region at the back surface of a solar cell creates a high-low junction. Therefore this characterized region will be named back surface field (BSF) in the following.

Further details concerning the post-treatments can be found in [13].

A drawback of the technique is the technical difficulty to align the sawing and the subsequent polishing to a series of lined up contacts and, at the same time, to realize a cut along the maximum extension of the contacts. Therefore, when analyzing the stain etched stratification on SEM images, it is to be considered that projections of the real layer thickness are observed. However, the expected angle deviation amongst the polishing performed is low. Therefore all the measurements of the thickness, even if not absolute, can be correctly compared with each other. Typically 5 to 8 local contacts from each sample have been investigated.

## 3. RESULTS

### 3.1 Classification of the contact formations

During the characterization three major typologies of contacts were identified as shown in Figure 5: a triangle (1), a geometrical shape close to a trapezium (2) and a third waved configuration characterized by having rounded edges at the side of the contact. Furthermore, all the hybrid shapes showing at least one straight lateral edge have been considered in the trapezoidal group. In addition, for larger widths of the trapezoidal contacts, the lower side of the trapezium can result in a particularly rounded shape. In some cases all these three different profiles have been observed in the same specimen where several polishing steps were realized.

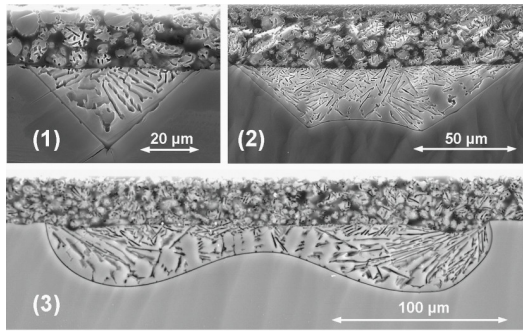


**Figure 5:** SEM cross sectional micrographs of the three major profiles noticed during the characterization: triangular (1), trapezoidal (2) and waved profile with rounded edges (3).

Figure 6 and Figure 7 show how the thickness of the BSF (respectively min and max) relates to the width of the contacts and to their cross sectional profile. For all the local contacts within a single specimen, both minimum and maximum thicknesses of the formed BSF were measured. Both diagrams refer to local contacts which were processed with different thermal profiles. The controlling parameters during the firing were both peak temperature and cooling down ramp. Two different pastes were screen printed at the back surface.

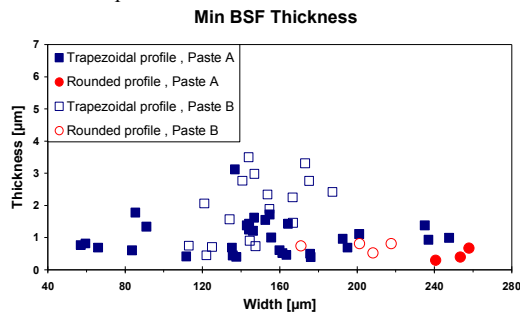


**Figure 6:** Plot of the min BSF thickness as a function of the measured width and the shape of the contacts.

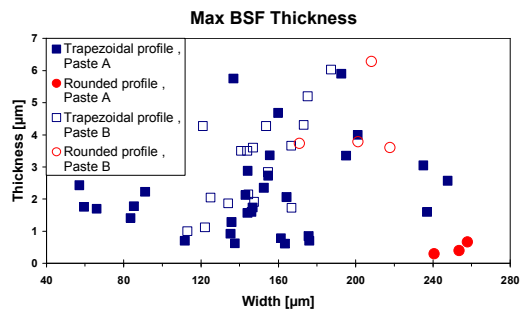


**Figure 7:** Plot of the max BSF thickness as a function of the measured width and the shape of the contacts.

The profile indicated as “trapezoidal” in diagrams above refers to the configuration (1) and (2) of Figure 5. The reason of this unification will be explained in the following. The profile named “rounded” identifies the family of contacts indicated as (3) in Figure 5. The different pastes are also indicated in the graphs.

From the graphs, two results are worth to underscore:

- Independently from the paste, contacts with a

rounded profile are formed when the width of the contact is larger than 160 μm. For such contacts, up to 6 μm maximum values of the BSF are measured for Paste B. Concerning the minimum value of the BSF, comparable behaviours are observed for both the pastes.

- In average both minimum and maximum BSF layers are thicker when Paste B is considered. In particular the influence of this latter paste on the minimum value of the BSF turns out to be relevant for contacts having widths in the range of 120 to 190 μm.

### 3.2 Homogeneity of the doped region

The plot of the maximum values of the BSF as a function of the minimum ones is shown in Figure 8. This diagram focuses on the trapezoidal distributions. In this regard, since the configuration referred to as “rounded” occurs for widths of the contacts larger than 160 μm, these profiles have not been taken into account. In fact, with such widths, very large distances between the contacts are needed in order to realize a constant metallisation fraction on the back surface.

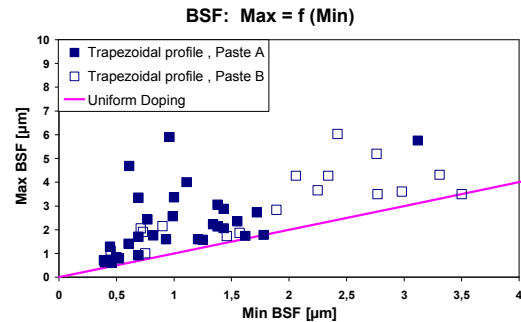


**Figure 8:** Plot of the maximum values of the BSF as a function of the minimum ones for each local contact analyzed. The “uniform doping” indicates ideal local contacts having a constant BSF thickness.

## 4. DISCUSSION

The difference in shape observed for the analyzed contacts is evident (see Figure 5) even though it needs to be further discussed to explain its origin.

According to [10], pyramidal contacts are observed when alloying aluminium and {100} mono-crystalline silicon in a high temperature process for screen printed metallization on passivation layers which are locally laser-opened.

For the symmetry observed in the local contacts analyzed in this study and considering that triangular shapes are always observed for smaller widths of the contacts, it was gathered that the contacts have geometrical shapes close to frustums.

Figure 9 sketches what kind of cuts have to be realized in order to obtain either triangular (a) or trapezoidal (b) profiles in the cross sections of the contacts.

The cut (red dashed line) occurs in a direction which is parallel to one of the axis of symmetry of the opened windows. As mentioned before, these latter windows are aligned to the edge of the wafer and not to the cleaving axis of the wafers. Because of that, the orientation of the base of the pyramid differs from the orientation of the opening in the passivation layer and, when sawing, different symmetric profiles of the contacts can be

displayed in the realized cross sections.

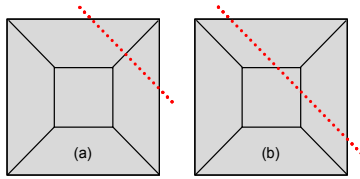


**Figure 9:** Sketch not in scale of the top view of a local contact. The dashed red lines indicate the direction of the sawing.

The waved profile with rounded edges (configuration (3) in Figure 5) is expected to be observed when cross sectioning local contacts with widths larger than 170  $\mu\text{m}$ . For such contacts the formed alloy is expected to extend underneath the passivation.

Concerning the diagrams of Figure 6 and Figure 7, it was observed that the two different pastes considered in the analysis and consisting of pure aluminium particles (i.e. without any glass frits or other compounds) behave differently in terms of BSF formation as a function of the width of the contacts. In addition, from the diagram in Figure 8 it is gathered that Paste B is to be preferred because it allows forming thicker and more homogeneous BSF layers.

## 5. CONCLUSIONS

In this study an optical characterization of local aluminium BSF has been offered for screen printed point like contacts structured with Inkjet contacting technique. Different variables have been considered in the analysis, i.e. different screen printable Al-pastes and a thermal firing variation. It was shown that different configurations of local contacts can be obtained as a function of the measured width of the contacts. From the results achieved, it turns out that Paste B contributes to the formation of a thicker and more homogenous BSF layer. As a consequence, Paste B is to be preferred for the realization of PERC solar cells.

The characterization developed in this study, if matched with electrical measurement of the resistivity of the contacts, can contribute significantly to optimize the performance of PERC solar cells.

## 6. ACKNOWLEDGEMENTS

The authors would like to thank Aleksander Filipovic and Mirosława Kwiatkowska for their precious aid at post-treating the samples.

## REFERENCES

[1] C. del Canizo, G. del Coso, and W. C. Sinke, "Crystalline silicon solar module technology: towards the 1€ per watt-peak goal", *Progress in Photovoltaics: Research and Applications*, vol. 17, pp. 199-209, 2009.

[2] L. Gautero, M. Hoffmann, J. Rentsch, B. Bitnar, J.-M. Sallse, and R. Preu, "All-screen-printed 120- $\mu\text{m}$ -thin large-area silicon solar cells applying dielectric rear passivation and laser-fired contacts reaching 18% efficiency", presented at Proceedings of the 24th European Photovoltaic Solar Energy Conference, Hamburg, Germany, 2009.

[3] J. Specht, D. Biro, N. Mingirulli, M. Aleman,

U. Belledin, R. Efinger, D. Erath, L. Gautero, A. Lemke, D. Stüwe, J. Rentsch, and R. Preu, "Using hotmelt-inkjet as a structuring method for higher efficiency industrial silicon solar cells", presented at Proceedings of the International Conference on Digital Printing Technologies and Digital Fabrication, Pittsburgh, PA, USA, 2008.

[4] R. Preu, S. W. Glunz, S. Schäfer, R. Lüdemann, W. Wettling, and W. Pflöging, "Laser ablation - a new low-cost approach for passivated rear contact formation in crystalline silicon solar cell technology", presented at Proceedings of the 16th European Photovoltaic Solar Energy Conference, Glasgow, UK, 2000.

[5] E. Schneiderlöchner, R. Preu, R. Lüdemann, and S. W. Glunz, "Laser-fired rear contacts for crystalline silicon solar cells", *Progress in Photovoltaics: Research and Applications*, vol. 10, pp. 29-34, 2002.

[6] F. Huster, "Investigation of the alloying process of screen printed aluminium pastes for the BSF formation on silicon solar cells", presented at Proceedings of the 20th European Photovoltaic Solar Energy Conference, Barcelona, Spain, 2005.

[7] C. T. Sah, F. A. Lindholm, and J. G. Fossum, "A high-low junction emitter structure for improving silicon solar cell efficiency", *IEEE Transactions on Electron Devices*, vol. 25, pp. 66-7, 1978.

[8] M. A. Green, *Solar cells: operating principles, technology and system applications*. Kensington: The University of New South Wales, 1998.

[9] P. Lölgen, "Surface and volume recombination in silicon solar cells", in *Faculteit der Natuur- en Sterrenkunde*. Den Haag: Universit t Utrecht, 1995, pp. 152.

[10] A. Uruena, J. John, G. Beaucarne, P. Choulat, P. Eyben, G. Agostinelli, E. Van Kerschaver, J. Poortmans, and M. R., "Local Al-Alloyed Contact for Next Generation Si Solar Cells", presented at 24th European Photovoltaic Solar Energy Conference, Hamburg, 2009.

[11] G. Beaucarne, P. Choulat, Y. Ma, F. Dross, A. Uruena, G. Agostinelli, J. Szlufcik, and J. John, "Local Al-Alloyed Contacts for next generation Si solar cells", presented at Workshop on Metallization for Crystalline Silicon Solar Cells, Utrecht, 2008.

[12] J. Nekarda, S. Stumpp, L. Gautero, M. H rteis, A. Grohe, D. Biro, and R. Preu, "LFC on screen printed aluminium rear side metallization", presented at Proceedings of the 24th European Photovoltaic Solar Energy Conference, Hamburg, Germany, 2009.

[13] F. S. Grasso, L. Gautero, J. Rentsch, R. Preu, and R. Lanzafame, "Characterization of aluminium screen-printed local contacts", presented at Proceedings of the 2nd Workshop Metallization for Crystalline Silicon Solar Cells, Constance, Germany 2010.

[14] S. Narasimha, A. Rohatgi, and A. W. Weeber, "An optimized rapid aluminum back surface field technique for silicon solar cells", *IEEE Transactions on Electron Devices*, vol. 46, pp. 1363-70, 1999.

[15] W. R. Runyan, *Semiconductor Measurements and Instrumentation*. New York: Mc Graw Hill, 1975.

[16] E. Urrejola, K. Peter, H. Plagwitz, and G. Schubert, "Al-Si alloy formation in narrow p-type Si contact areas for rear passivated solar cells", *Journal of Applied Physics*, vol. 107, pp. 124516, 2010.